BJP British Journal of Pharmacology

DOI:10.1111/bph.12817
www.brjpharmacol.org

RESEARCH PAPER

An *in vivo* role for Rho kinase activation in the tumour vascular disrupting activity of combretastatin A-4 3-*O*-phosphate

L J Williams*‡, D Mukherjee*, M Fisher*, C C Reyes-Aldasoro§, S Akerman¶, C Kanthou† and G M Tozer†

Tumour Microcirculation Group, Sheffield Cancer Research Centre, Department of Oncology, School of Medicine, The University of Sheffield, Sheffield, UK

Correspondence
Gillian M Tozer, Tumour Microcirculation Group, Sheffield Cancer Research Centre, The University of Sheffield, Department of Oncology, F Floor, School of Medicine, Beech Hill Road, Sheffield S10 2RX, UK.
E-mail: g.tozer@sheffield.ac.uk

*These authors contributed equally to the work.

†Joint senior authors.

‡Current address: AstraZeneca, Alderley Park, Cheshire, UK.

§Current address: School of Engineering and Mathematical Sciences, City University, London EC1V OHB, UK.

¶Current address: Department of Neurology, University of California, San Francisco, 675 Nelson Rising Lane, San Francisco, CA 94158, USA.

Received
30 September 2013
Revised
29 April 2014
Accepted
2 June 2014

BACKGROUND AND PURPOSE

Combretastatin A-4 3-*O*-phosphate (CA4P) is in clinical trial as a tumour vascular disrupting agent (VDA) but the cause of blood flow disruption is unclear. We tested the hypothesis that activation of Rho/Rho kinase (ROCK) is fundamental to the effects of this drug *in vivo*.

EXPERIMENTAL APPROACH

Mouse models of human colorectal carcinoma (SW1222 and LS174T) were used. Effects of the ROCK inhibitor, Y27632, alone or in combination with CA4P, on ROCK activity, vascular function, necrosis and immune cell infiltration in solid tumours were determined. Mean arterial BP (MABP) was measured to monitor systemic interactions and the vasodilator, hydralazine, was used to control for the hypotensive effects of Y27632.

KEY RESULTS

Y27632 caused a rapid drop in blood flow in SW1222 tumours, with recovery by around 3 h, which was paralleled by MABP changes. Y27632 pretreatment reduced CA4P-induced ROCK activation and partially blocked CA4P-induced tumour vascular effects, in both tumour types. Y27632 also partially inhibited CA4P-induced tumour necrosis and was associated with reduced immune cell infiltration in SW1222 tumours. Hydralazine caused a similar hypotensive effect as Y27632 but had no protective effect against CA4P treatment.

CONCLUSIONS AND IMPLICATIONS

These results demonstrate that ROCK activity is critical for full manifestation of the vascular activity of CA4P *in vivo*, providing the evidence for pharmacological intervention to enhance the anti-tumour efficacy of CA4P and related VDAs.

Abbreviations

CA4P, combretastatin A-4 3-*O*-phosphate; CD31, platelet endothelial cell adhesion molecule; eNOS, endothelial NOS; HPA, Health Protection Agency; I-R, ischaemia-reperfusion; MABP, mean arterial BP; MPO, myeloperoxidase; p-ERM, phosphorylated ezrin-radixin-moesin; Rho, Rho-GTPase; ROCK, Rho kinase; SCID, severe combined immunodeficiency; VDA, vascular disrupting agent

Table of Links

TARGETS	LIGANDS
NO synthase (NOS)	Hydralazine
Rho kinase (ROCK)	Y27632

This Table lists key protein targets and ligands in this article which are hyperlinked to corresponding entries in http://www.guidetopharmacology.org, the common portal for data from the IUPHAR/BPS Guide to PHARMACOLOGY (Pawson *et al.*, 2014) and are permanently archived in the Concise Guide to PHARMACOLOGY 2013/14 (Alexander *et al.*, 2013).

Introduction

Colchicine-related microtubule depolymerizing agents are the largest family of low MW drugs to have tumour vascular disrupting activity at relatively non-toxic doses (Tozer *et al.*, 2005; Kanthou and Tozer, 2007; Siemann, 2011). Combretastatin A-4 3-*O*-phosphate (CA4P or fosbretabulin/Zybrestat; Pettit *et al.*, 1989; 1995) was the first of this class of vascular disrupting agents (VDAs) to enter clinical trials (Dowlati *et al.*, 2002; Rustin *et al.*, 2003). Preclinical studies showed that anti-tumour activity of CA4P was dependent on dose, scheduling, tumour type and vascular characteristics (Boehle *et al.*, 2001; Hill *et al.*, 2002; Tozer *et al.*, 2008a), with particular efficacy in combination with conventional chemotherapy or radiotherapy (Murata *et al.*, 2001b; Siemann *et al.*, 2002). CA4P has progressed to phase II trials in patients with relapsed ovarian cancer and to phase III trials in patients with anaplastic thyroid cancer, primarily in combination with conventional chemotherapy (http://www.oxigene.com/product-development/zybrestat).

Shortly after administration *in vivo*, CA4P is cleaved to the active form, CA4, (Stratford and Dennis, 1999), which has been shown to bind β-tubulin resulting in microtubule destabilization and net depolymerization (McGown and Fox, 1989). The effects of well-tolerated doses of CA4P *in vivo* are evident almost immediately by a rapid and selective decrease and loss of tumour blood flow, which becomes maximal between 1 and 4 h after administration and can remain lowered in both animal and human tumours for up to 24 h before vasculature re-establishes itself (Dark *et al.*, 1997; Murata *et al.*, 2001a; Prise *et al.*, 2002; Galbraith *et al.*, 2003). Central tumour necrosis is apparent within 24 h of treatment accompanied by leucocyte infiltration into the tumour mass. Tumour-infiltrating Tie2-positive macrophages act to reduce CA4P-induced tumour vascular injury or to aid recovery of the vasculature following drug exposure (Welford *et al.*, 2011). A similar effect was ascribed to endothelial progenitor cells, mobilized from the bone marrow by a second-generation combretastatin, combretastatin A-1 diphosphate (Oxi4503; Shaked *et al.*, 2006). Myeloperoxidase (MPO) accumulation in CA4P-treated tumours (Parkins *et al.*, 2000) also suggested a role for neutrophils in determining the ultimate fate of tumour cells following VDA treatment.

In endothelial cells *in vitro*, CA4-induced depolymerization of interphase microtubules is accompanied by generation of actinomyosin contractility and reorganization of the actin cytoskeleton through activation of Rho-GTPase (Rho)/Rho kinase (ROCK) and MAPK signalling (Kanthou and Tozer, 2002). Indeed, actin stress fibres and focal adhesions form very rapidly after treatment with CA4P while some endothelial cells assume a rounded 'blebbing' morphology, probably through increased contractility as well as elevated p38 SAPK activity (Kanthou and Tozer, 2002). Disruption of cell–cell junctions leading to gap formation and increased monolayer permeability to macromolecules is also a feature of the early response of endothelial cells to CA4P driven by Rho/ROCK (Kanthou and Tozer, 2002; Vincent *et al.*, 2005). Additionally, the rounding of endothelial cells and the loss of cell-to-cell adhesions was shown to be associated with CA4P inhibition of vascular endothelial cadherin and β-catenin complexes and the inhibition of the PI3K/Akt pro-survival signalling pathway (Vincent *et al.*, 2005). Blood flow disruption in solid tumours is accompanied by an increase in vascular permeability to macromolecules (Reyes-Aldasoro *et al.*, 2008), paralleling effects observed for endothelial cells *in vitro* and suggesting that knowledge gained from *in vitro* studies is useful for deciphering mechanisms associated with drug activity *in vivo*.

Activation of Rho/ROCK signalling following CA4P administration *in vitro* was established using inhibitors such as recombinant C3 exoenzyme of clostridium botulinum that inhibits Rho and the ROCK inhibitor Y27632 (Kanthou and Tozer, 2002). These studies showed that the increase in endothelial cell monolayer permeability, as well as the morphological changes induced by CA4P *in vitro*, was Rho/ROCK dependent. Establishing the links between Rho/ROCK signalling activation and cytoskeletal effects of CA4P in endothelial cells has advanced an understanding of the mechanism of

action of CA4P. However, whether there is any involvement of Rho signalling in the mechanism of action of CA4P *in vivo* is unknown. The ROCK inhibitor, Y27632, was originally developed as an anti-hypertensive agent (Uehata *et al.*, 1997). This compound has been extensively used *in vivo* to demonstrate key roles of ROCK in many other processes including inflammation and ischaemia-reperfusion (I-R) injury (Bao *et al.*, 2004; Hamid *et al.*, 2007). Using this agent, the aim of the current study was to determine the role of the Rho/ROCK signalling pathway in CA4P-induced vascular shutdown, necrosis induction and leucocyte infiltration in two human colorectal xenografted tumour models in mice. We controlled for the potent hypotensive effect of Y27632 by comparing its effects with those of the direct vasodilator, hydralazine (Sawada *et al.*, 2000; Wang *et al.*, 2008). We found a protective effect of Y27632 but not hydralazine against CA4P, demonstrating an important role for ROCK activity in the mechanism of action of this tumour VDA *in vivo*.

Materials and methods

Cell systems

The human colorectal carcinoma cell lines SW1222 (kindly provided by Dr R B Pedley, University College London) and LS174T (European Collection of Cell Cultures) were maintained in DMEM supplemented with 10% foetal calf serum, 100 U mL^{-1} penicillin, 100 μg mL^{-1} streptomycin and 2 mM L-glutamine (Lonza, Cambridge UK).

The purity of the SW1222 cell line was verified by routinely checking for its characteristic glandular morphology, when established *in vivo* (Richman and Bodmer, 1988) and by performing PCR-based microsatellite genotyping analysis [Health Protection Agency (HPA), UK]. Fingerprint baseline information was not available for the SW1222 line. However, the generated profile of the SW1222 cells was unique when compared with profiles of all human cell lines in the HPA database. LS174T cells were used at early passages only.

Animals and tumours

All animal care and experimental procedures were carried out in accordance with the UK Animals (Scientific Procedure) Act 1986, with local ethics committee approval and following published guidelines for the use of animals in cancer research (Workman *et al.*, 2010). All studies involving animals are reported in accordance with the ARRIVE guidelines for reporting experiments involving animals (Kilkenny *et al.*, 2010; McGrath *et al.*, 2010). A total of 336 animals were used in the experiments described here.

Mice were provided with regular mouse chow and water *ad libitum* and kept on a 12 h light/dark cycle. Tumour cells (5×10^6 in non-supplemented DMEM) were implanted subcutaneously onto the rear dorsum of mixed sex 8–12-week-old severe compromised immune-deficient (SCID) mice. Tumours were selected for treatment 12–20 days post-implantation, when the geometric mean diameter reached 6–7 mm.

Drug treatment

All drugs were administered i.p. at 10 mL kg^{-1} in physiological saline. Mice were killed at 1, 3, 6 or 24 h after single-dose CA4P treatment (OxiGene Inc., San Francisco, CA, USA), at 100 mg kg^{-1}; a previously determined effective dose for SW1222 tumours (Lunt *et al.*, 2011). Y27632 (Tocris Bioscience, Bristol, UK) was administered at the maximum tolerated dose in our mice of 50 mg kg^{-1} (unpublished data), either alone or 5 min before or 3 h after CA4P treatment. Twice daily doses of 50 mg kg^{-1} Y27632 have been used previously in mice (Mavria *et al.*, 2006). Hydralazine (Sigma-Aldrich Co Ltd, Gillingham, UK) was administered at 2 mg kg^{-1}, either alone or 5 min before CA4P treatment, to induce a similar hypotensive effect to that of Y27632 (Sawada *et al.*, 2000; Wang *et al.*, 2008).

Arterial BP

The effect of drug treatment on mean arterial BP (MABP) in unanaesthetized, non-tumour-bearing mice was measured via an occlusion and plethysmograph tail cuff system (Kent Scientific Corporation, Torrington, CT, USA). Mice were acclimatized to the equipment for a minimum of 1 h·day^{-1} for 7 days prior to drug treatments. MABP was calculated as [(diastolic pressure ×2) + systolic pressure]/3. MABP in mmHg was recorded in triplicate before and at various times up to 24 h after i.p injection of Y27632 ± CA4P, with relevant saline controls. Values were averaged for each time point.

Laser Doppler flowmetry

In order to monitor acute effects of drug treatments in individual animals, relative changes in volumetric tumour microvascular red cell flux were measured using the Oxyflo™ laser Doppler perfusion system (Oxford Optronix Ltd, Oxford, UK). Mice were anaesthetized with isoflurane (maintenance dose of 1.5–2.0% in oxygen) and maintained on a thermostatically controlled heating pad throughout. Up to four probes of <1 mm diameter were inserted into the tumour at various depths. Once readings were stable (approximately 20 min), mice were injected i.p with Y27632 (50 mg kg^{-1}) or vehicle control (saline) and readings taken for a further 5 minute period. Animals were then injected i.p with CA4P (100 mg kg^{-1}) or vehicle control (saline) and readings taken for a further 120 min, followed by killing of the animals by an i.v. overdose of sodium pentobarbitone. *Post mortem* baseline readings for each probe were subtracted from probe readings obtained throughout the experiment. Data were expressed as a percentage of the pretreatment value.

Perfusion index

Mice were treated as above and the tumour perfusion index calculated at 1, 3, 6 or 24 h after CA4P, as published previously (Lunt *et al.*, 2011). Briefly, 0.2 mg FITC-conjugated *Lycopersicon esculentum* tomato lectin (Vector Laboratories, Peterborough, UK) per mouse was injected 5 min before killing to detect perfused blood vessels at the time of lectin injection. Excised tumours were rapidly frozen and cryosections immuno-stained for platelet endothelial cell adhesion molecule (CD31), using Alexa-Fluor 555 for visualization, to detect both perfused and unperfused blood vessels. Detailed methods for staining and image capture are described in Supporting Information Appendix S1.

Individual captured images were analysed using in-house-developed Matlab-based software. Fluorescence channels

were manually thresh-holded for each individual tumour. The perfusion index for each image was calculated as the number of pixels positive for FITC as a percentage of the number of pixels positive for Alexa-Fluor 555.

Histology and immunohistochemistry

Tumours from animals culled at 24 h after treatment were fixed, sectioned and stained with haematoxylin and eosin for necrosis scoring, immuno-stained for MPO for identification of neutrophils or immuno-stained for the phosphorylated form of the ROCK substrate protein complex ezrin-radixin-moesin (p-ERM) as a marker of ROCK activation (Matsui *et al.*, 1998).

Necrosis was scored according to a random points scoring system. Whole tumour sections were scanned using an eyepiece graticule marked with 25 random points (Chalkley grid) and a ×20 objective. Approximately 150 regions were scanned per tumour. Necrosis was identified by reduced cellular density, pale cytoplasm and pyknotic nuclei or completely disrupted cells. The number of points falling on necrotic tissue as a % of total points counted was used to calculate necrosis as a % of the total sectional area.

A rabbit anti-mouse polyclonal antibody (Dako, Ely, UK; 1:150 dilution) was used for MPO staining, as described in detail in Supporting Information Appendix S1. A Chalkley grid was used, as described above, for scoring MPO in necrotic areas, where staining was widespread. A squared eyepiece grid and a ×20 objective were used for scoring MPO in viable tissue areas, where staining was sparse. The grid was systematically moved across viable areas and all positive-stained cells were counted within the grid. Necrotic and viable scores were combined to calculate the total MPO staining as a % of the total tumour section area.

A rabbit monoclonal antibody (Cell Signaling, Hertfordshire, UK) was used to detect p-ERM, as described in Supporting Information Appendix S1. Sections were scanned and p-ERM staining was calculated as % of total viable section area using the Scanscope CS® system (Aperio, Vista, CA, USA).

Data analysis

Results are shown as means ± SEM. Statistical analysis was carried out using GraphPad Prism software Version 5.0d for Macintosh (GraphPad Software Inc., San Diego, USA). MABP and laser Doppler data were analysed using a two-way ANOVA with repeated measures followed by a Bonferroni *post hoc* test. Perfusion index data for SW1222 tumours determined at different time points after CA4P treatment were analysed by a two-way ANOVA followed by a Bonferroni *post hoc* test. Student's *t*-test (for comparison of two groups) or a one-way ANOVA followed by a Bonferroni or Newman–Keuls *post hoc* test (for comparison of more than two groups) were used for all other data sets. In all cases, differences between treatment groups were described as significant if the probability corresponding to the relevant statistic was less than 0.05.

Results

Efficacy of Y27632 in solid tumours in vivo

In order to determine the efficacy of the ROCK inhibitor Y27632 *in vivo*, we used p-ERM as a marker for ROCK activation (Hamid *et al.*, 2007). Figure 1 shows that p-ERM in control saline-treated SW1222 tumours was primarily detected in the stroma, most likely associated with endothelial cells, where moesin is known to be the most prevalent of this specialized family of proteins (Fehon *et al.*, 2010). Treatment with CA4P caused a marked increase in the intensity and pervasiveness of p-ERM staining both in the stroma and on tumour cells (Figure 1). Staining of tumour cells was confined to the cell periphery, consistent with the known location of ERM proteins on cell membranes, where they interact with trans-membrane proteins and the cytoskeleton to control a diverse range of cellular functions (Fehon *et al.*, 2010). Y27632 alone had no effect on p-ERM expression (Figure 1) but pretreatment with Y27632 blocked the increase in p-ERM expression observed for CA4P treatment administered alone (Figure 1).

Systemic effects

Y27632 is a hypotensive agent, acting on vascular smooth muscle cells and the sympathetic nervous system (Ito *et al.*, 2003; Moosmang *et al.*, 2003). In order to control for these effects, we also used hydralazine, a direct acting vascular smooth muscle relaxant that has been used previously for similar purposes (Sawada *et al.*, 2000) (Wang *et al.*, 2008). Figure 2A shows that Y27632 and hydralazine, at the chosen doses, had similar and rapid hypotensive effects. CA4P alone caused a small increase in MABP (Figure 2A), which is consistent with previous results for both rat and man (Galbraith *et al.*, 2003). It should be noted that 100 mg kg^{-1} CA4P has been used commonly in mice but, on a body surface area basis, this is approximately four times the maximum tolerated dose in man (Rustin *et al.*, 2003). Doses of around 10 mg kg^{-1} have activity in rodent models of cancer (Prise *et al.*, 2002) but our aim here was to ensure we achieved a profound CA4P-induced tumour vascular response for meaningful testing of the ROCK inhibitor, Y27632. The combination of either Y27632 or hydralazine with CA4P dropped MABP to similar levels as Y27632 or hydralazine alone but return to control levels was somewhat delayed for both combination groups (Figure 2A). By 24 h after treatment, MABP was the same for all groups, with no obvious signs of toxicity.

Effects of ROCK inhibition on tumour vascular disrupting properties of CA4P

Early tumour vascular effects were first studied in SW1222 tumours using laser Doppler flowmetry. Figure 2B) shows a similar and substantial drop in red cell flux to approximately 40% of pretreatment levels for both Y27632 and CA4P administered as single agents. The time course of the decrease for Y27632 alone was significantly different from the control group by 5 min after administration and very similar to that for MABP (Figure 2A), implicating a decrease in perfusion pressure as the stimulus for blood flow reduction. The reduction in tumour red cell flux following CA4P treatment was somewhat slower than for Y27632 (significantly different from the control group by 20 min after administration) but reached similar low levels by 30–40 min, with a further slow decline during the remaining time course of the experiment. In this case, as reported previously (Tozer *et al.*, 1999; Ke *et al.*, 2009), the blood flow effects could not be explained by a

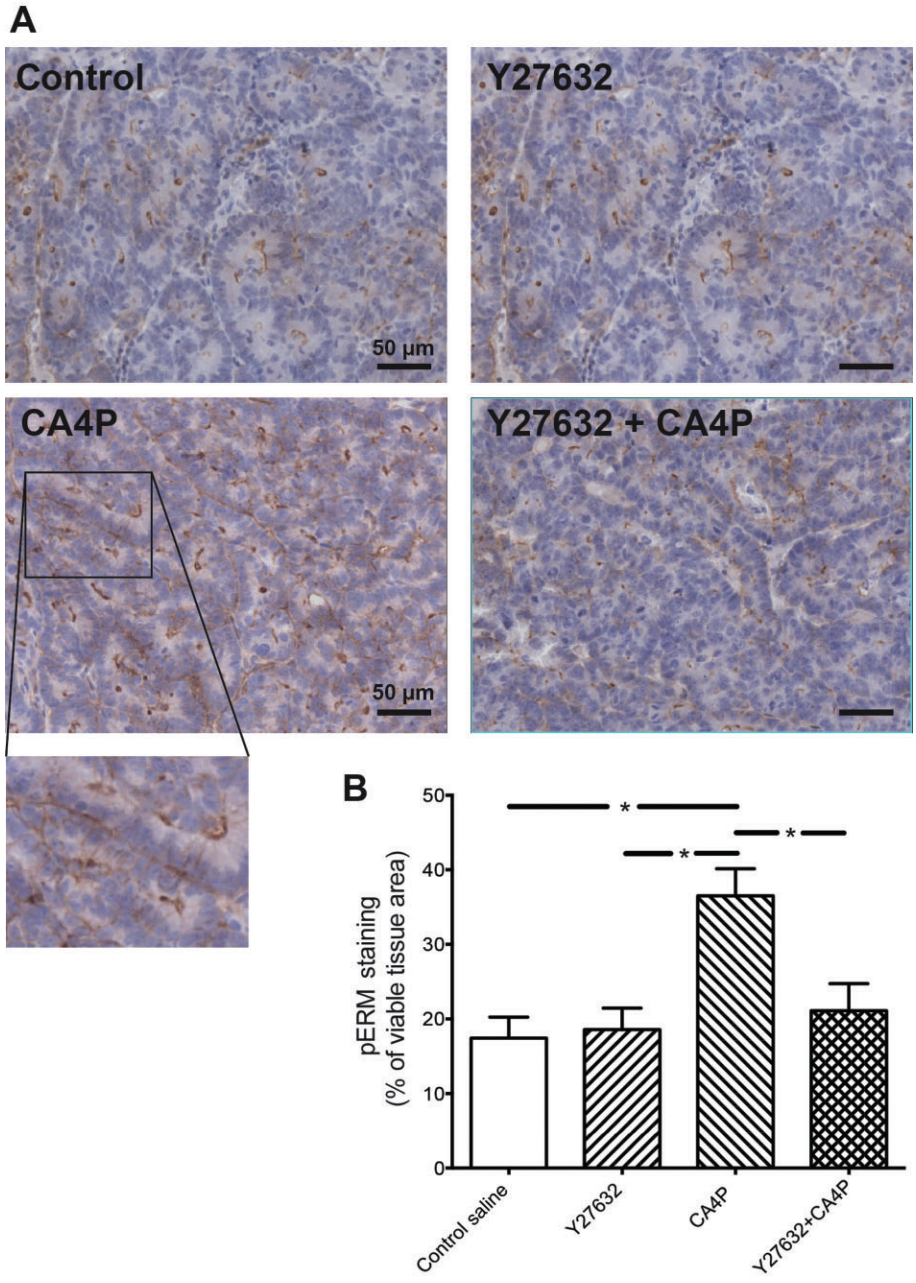

Figure 1

(A) Representative staining images for p-ERM in control saline-treated SW1222 tumours; 24 h after Y27632 (50 mg kg^{-1}) alone; 24 h after CA4P (100 mg kg^{-1}) treatment alone; 24 h after combination of Y27632 administered 5 min prior to CA4P. CA4P treatment resulted in more intense and pervasive staining, especially in cell membranes of tumour cells, as shown in the magnified inset. Y27632 treatment alone and the combination treatment resulted in moderate levels of staining comparable to control. (B) Quantification data for all the four groups. Columns represent mean ± SEM for n = 8–11 mice per group. *P < 0.05, significant difference between groups (one-way ANOVA with Bonferroni post test).

decrease in perfusion pressure, as CA4P caused a moderate hypertensive effect, when administered as a single agent (Figure 2A). Combination of Y27632 and CA4P resulted in a sustained decrease in red cell flux that was almost identical to that for Y27632 alone, with no indication of any additive effect. There was no statistical difference in red cell flux between the three drug-treated groups by the end of the experiment (2 h after drug administration).

Figure 3A shows representative images for FITC-lectin and CD31 staining in frozen sections of SW1222 tumours, following *in vivo* administration of CA4P or vehicle ± Y27632. Figure 3B (left panel) shows the calculated perfusion index (FITC-lectin staining as a % of CD31 staining) from 1 to 24 h following *in vivo* administration of CA4P or vehicle ± Y27632. Results show that the tumour perfusion index following Y27632 treatment alone had returned to control levels by 3 h,

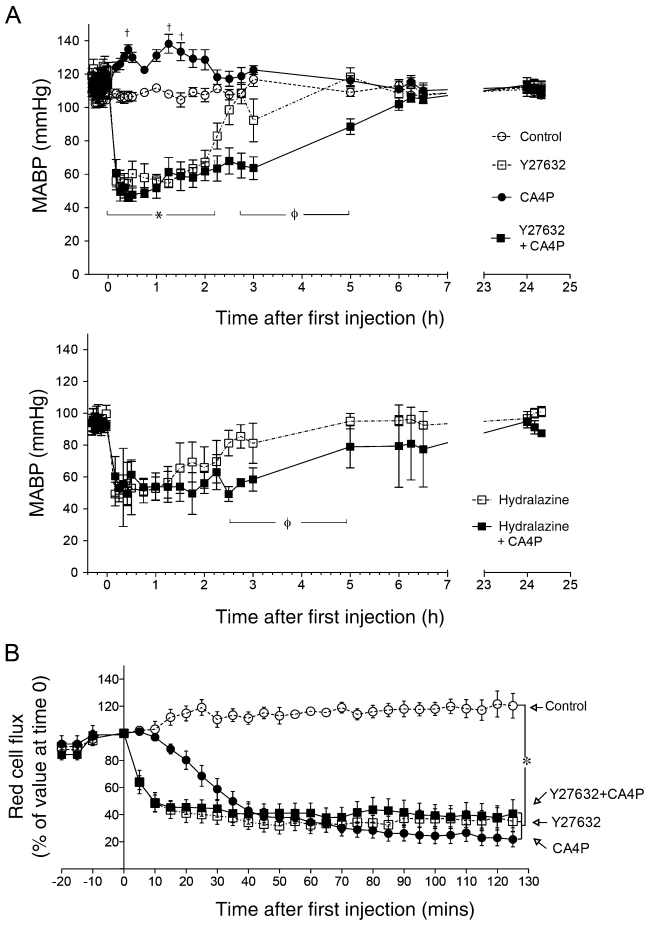

Figure 2

(A) MABP measured by tail cuff plethysmography in conscious restrained severe compromised immune-deficient mice. Open circles, control saline treated; closed circles, CA4P (100 mg kg^{-1} i.p.); open squares in upper panel, Y27632 (50 mg kg^{-1} i.p.); closed squares in upper panel, Y27632 (50 mg kg^{-1} i.p.) administered 5 min prior to CA4P (100 mg kg^{-1} i.p.); open squares in lower panel, hydralazine (2 mg kg^{-1} i.p.); closed squares in lower panel, Y27632 (2 mg kg^{-1} i.p.) administered 5 min prior to CA4P (100 mg kg^{-1} i.p.). †$P < 0.05$, significant difference between individual data points in the CA4P group and the equivalent data points for the saline control group; two-way ANOVA with repeated measures. *$P < 0.05$, range over which there is a significant difference between the Y27632 and saline control group and between the Y27632 + CA4P group and the saline group; two-way ANOVA with repeated measures. Φ$P < 0.05$,range over which there is a significant difference between the Y27632 + CA4P group and the Y27632 alone group (upper panel) or the hydralazine + CA4P group and the hydralazine alone group (lower panel); two-way ANOVA with repeated measures. Each symbol represents mean ± SEM for 5–13 mice. (B) Tumour perfusion measured by laser Doppler flowmetry following the same treatments as in the upper panel of A. *$P < 0.05$, significant difference between the control saline group and all other groups at the end of the observation period; two-way ANOVA with repeated measures. No statistical difference was found between the CA4P alone, Y27632 alone and combination treatment groups at the end of the observation period (two-way ANOVA with repeated measures). Each symbol represents means ± SEM for six mice.

consistent with a recovery in perfusion pressure, as implied by the BP data shown in Figure 2A. The perfusion index following CA4P treatment alone declined steadily for at least 24 h, at which time lectin staining was only approximately 5% of CD31 staining. Pretreatment of CA4P-treated mice with Y27632 partially prevented the protracted decline in perfusion index found for CA4P alone, resulting in a perfusion index of 20% compared with approximately 10% for CA4P alone at 6 h and 20% compared with 5% for CA4P alone at 24 h. These differences were statistically significant. In contrast, administration of hydralazine prior to CA4P had no protective effect at 24 h (right-hand panel in Figure 3B). Administration of Y27632 3 h after CA4P had no protective effect on the perfusion index at 6 or 24 h post-CA4P treatment (Supporting Information Figure S1). Pretreatment with Y27632 had a similar protective effect in the LS174T tumour as in the SW1222 tumour, assayed at 24 h after CA4P treatment (Figure 3C). The perfusion index was partially and significantly maintained to approximately 20%, compared with approximately 5% for CA4P alone. However, unlike in the SW1222 tumour, no protective effect was apparent at 6 h after CA4P treatment.

Effects of ROCK inhibition on induction of tumour necrosis by CA4P

Figure 4 shows the effect of Y27632, CA4P and the combination treatment on necrosis induction at 24 h after CA4P treatment in the two tumour types. Figure 4A and B shows that necrosis in SW1222 tumours was less than 20% in control and Y27632-treated tumours, with no significant difference between necrosis levels in the two groups, whereas CA4P treatment significantly increased necrosis to more than 60%. Pretreatment with Y27632 partially blocked this effect, such that necrosis levels were below 40% and significantly different from levels in both control and CA4P-treated groups. However, as for the vascular effects shown in Figure 3, hydralazine had no effect on CA4P-induced tumour necrosis (Figure 4B). Administration of Y27632 3 h after CA4P also had no effect (Figure 4B). Figure 4C shows the equivalent results for the LS174T tumours. Control necrosis levels were very high in these tumours equating to approximately 60% of the sectional areas, with similar levels found for Y27632-treated tumours, and with no significant increase following CA4P treatment. No significant differences were found for necrosis levels between any of the treatment groups for this tumour type, despite the significant vascular effects shown in Figure 3.

Effects of ROCK inhibition on MPO expression following CA4P treatment

Very little MPO expression was detected in control untreated SW1222 tumours or the same tumours treated with Y27632 alone (≤0.1% of the sectional area; Figure 5A and B). There was significantly increased MPO expression, to approximately 1.5%, in SW1222 tumours 24 h after CA4P treatment but there was large variability in MPO expression between individual CA4P-treated tumours such that the apparent 50% reduction by prior treatment with Y27632 (Figure 5A and B) was only borderline significant (significant according to Newman–Keuls but not Bonferroni *post hoc* test). MPO

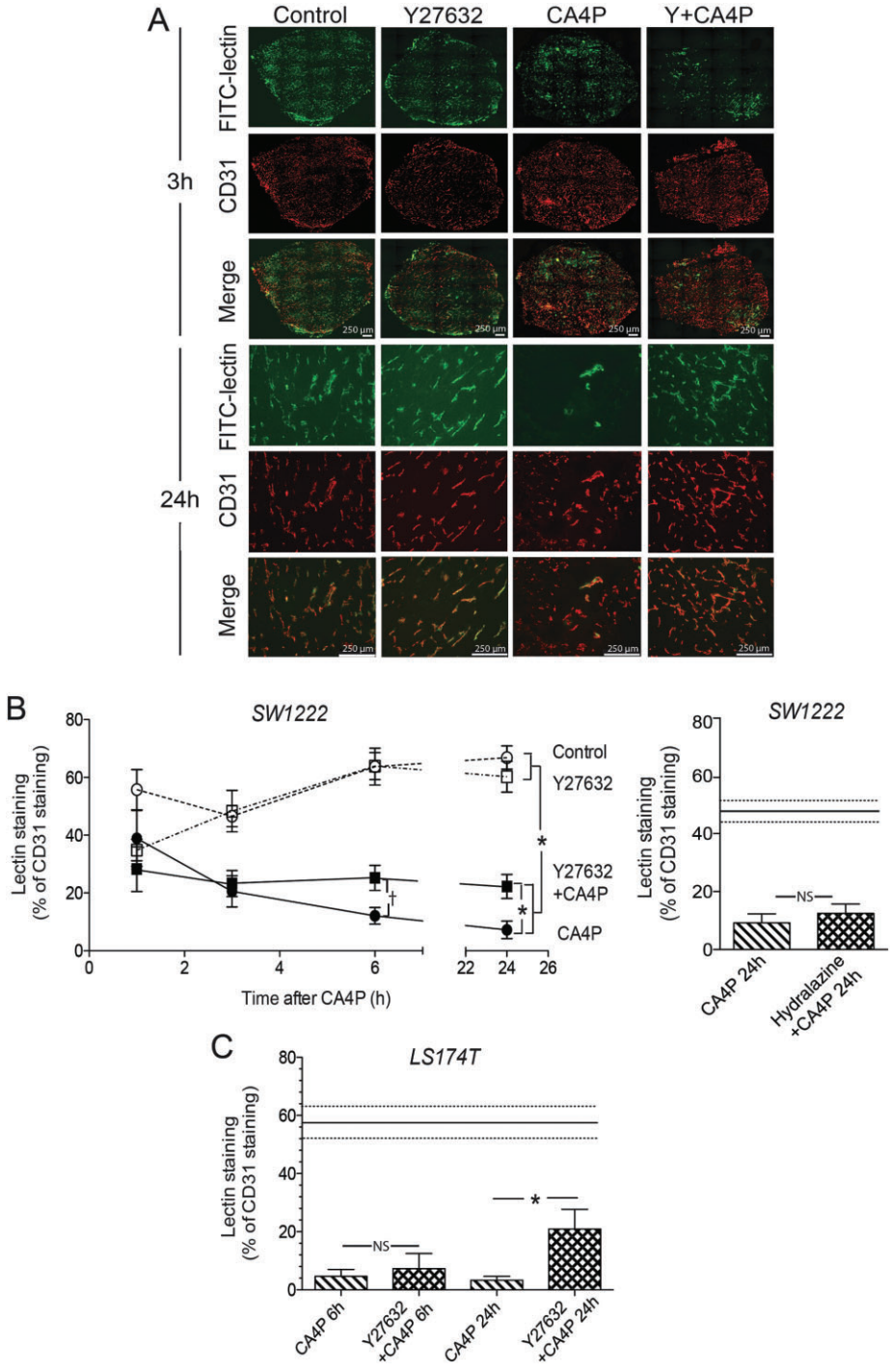

Figure 3

(A) Representative images of FITC-lectin and CD31 immuno-stained frozen sections from SW1222 tumours: untreated control, Y27632 (50 mg kg^{-1}) treatment alone, CA4P (100 mg kg^{-1}) treatment alone and the combination treatment (Y27632 5 min prior to CA4P). Tumours were excised at 3 or 24 h after CA4P or the relevant vehicle treatment and demonstrate lack of any effect of Y27632 at the early time point and a protective effect by 24 h. Scale bars represent 250 μm. (B) Perfusion index calculated as the number of pixels stained +ve for FITC-lectin as a % of the number of pixels stained +ve for CD31 for whole data sets in SW1222 tumours. A full time course is shown for the effect of Y27632 on CA4P-induced tumour vascular effects (left-hand panel; $n = 5–6$ for 1 and 3 hour time points; $n > 9$ for 6 and 24 h time points) and for 24 h after CA4P for the effect of hydralazine on CA4P-induced tumour vascular effects (right-hand panel; $n = 9$ for both groups). (C) Perfusion index calculated as above for the effect of Y27632 on CA4P-induced vascular effects in LS147T tumours at 6 and 24 h after CA4P. Points and bars represent means ± SEM for $n = 6–7$. The horizontal lines represent the mean ± SEM for control untreated tumours. *$P < 0.05$, in B, significant difference between groups for the full time course; †$P < 0.05$, significant difference at time = 6 h; two-way ANOVA. *$P < 0.05$, in C, significant difference between groups; one-way ANOVA with Bonferroni post test. NS represents a non-significant difference.

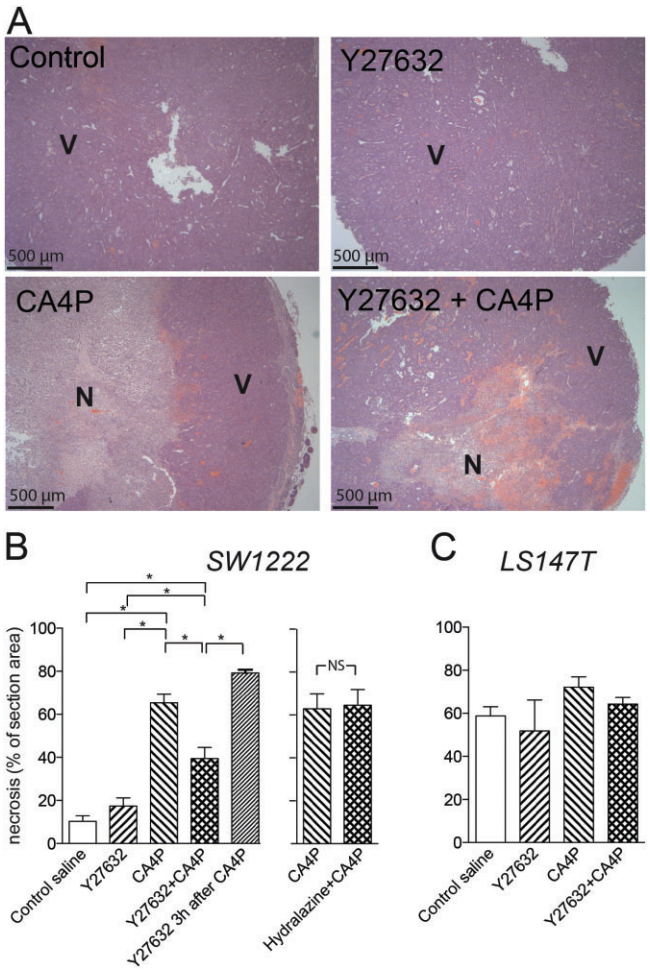

Figure 4

(A) Representative images of haematoxylin and eosin stained formalin-fixed sections from SW1222 tumours: untreated control, Y27632 (50 mg kg^{-1}) treatment alone, CA4P (100 mg kg^{-1}) treatment alone and the combination treatment (Y27632 5 min prior to CA4P). Tumours were excised at 24 h after CA4P or the relevant vehicle treatment. Scale bars represent 500 μm. N = necrosis; V = viable tumour region. (B) Quantification of necrosis in SW1222 tumours for the different treatments described above (left-hand panel) or for CA4P ± hydralazine 5 min prior to CA4P (right-hand panel), assayed at 24 h after CA4P or the relevant vehicle treatment. (C) Quantification of necrosis in LS147T tumours for the different treatments shown, assayed at 24 h after CA4P or the relevant vehicle treatment. Bars show means ± 1 SEM. *P < 0.05, significant difference between groups; one-way ANOVA followed by Bonferroni post test. n > 8 per group for SW1222; n > 4 per group for LS174T. NS represents a non-significant difference.

expression was primarily associated with necrotic tumour regions in both untreated and treated tumours, although there were also some isolated positively stained cells in viable tumour regions (white arrows in Figure 5A).

Discussion

Pretreatment administration of the ROCK inhibitor, Y27632, partially protected two types of colorectal carcinoma xenografts from the tumour vascular disrupting effects of the VDA, CA4P. In the SW1222 tumour, where CA4P treatment alone induced significant necrosis, this vascular protection was translated into a reduction in CA4P-induced necrosis. Administration of hydralazine, which replicated the hypotensive effect of Y27632, had no protective effect on CA4P-induced tumour vascular disruption or necrosis in SW1222 tumours, demonstrating that hypotension could not explain the protection found with Y27632. These results demonstrate that Rho-GTPase/ROCK activity is critical for full manifestation of CA4P's vascular activity *in vivo*.

Immuno-staining for p-ERM demonstrated that CA4-P induced the activation of ROCK in tumour tissue *in vivo*, confirming previous results for endothelial cells (Kanthou and Tozer, 2002) and SW1222 tumour cells (unpublished data) *in vitro*. Pretreatment with Y27632 was able to block the activation of ROCK induced by CA4P, as detected by p-ERM expression (Figure 1). Although not the focus of this study, the CA4P-induced increase in p-ERM expression within solid tumours is likely to be a significant step in the mode of action of this and similar tumour VDAs. The ERM proteins have diverse roles in cells, which are not fully understood. They are membrane-associated and interact with trans-membrane proteins, such as tyrosine kinase receptors, and various cell adhesion molecules to form complex membrane domains, which link to the underlying cytoskeleton for signal transduction (Fehon *et al.*, 2010). As well as mediating ROCK-activated remodelling of the F-actin cytoskeleton (Fehon *et al.*, 2010), interaction of specific ERMs with trans-membrane proteins is thought to be a requirement for their activity as co-receptors, for example, CD44 as a co-receptor for c-Met (Orian-Rousseau and Ponta, 2008). There is ample evidence from preclinical studies that CA4P is active against primary and metastatic disease (see Tozer *et al.*, 2005). However, the known roles of ROCK and activated ERMs in cell migration (Fehon *et al.*, 2010) suggest that, as well as having a central role in the mechanism of action of CA4P, CA4P-induced ROCK activity may also be involved in resistance pathways emanating from suboptimal CA4P dosing. Up-regulation of VEGF and other pro-angiogenic proteins have been observed following CA4P treatment (Boehle *et al.*, 2001; Sheng *et al.*, 2004; Shaked *et al.*, 2009) and ROCK activation is a key component of downstream VEGF signalling associated with migration and vascular permeability (van der Meel *et al.*, 2011). These observations are consistent with preclinical and clinical studies showing the benefit of following up a course of CA4P treatment with administration of the anti-VEGF antibody, bevacizumab (Siemann and Shi, 2008; Nathan *et al.*, 2012).

The protective effect of Y27632 against CA4P-induced vascular damage in SW1222 tumours was only manifested at relatively late times (6 and 24 h) after CA4P treatment (Figure 3A, B), despite administration of Y27632 just prior to CA4P and a profound effect of CA4P on tumour red cell flux and perfusion index within the first hour of treatment (Figure 2B and 3). A similar effect was observed for the LS174T tumour, at 24 h (Figure 3B). The fact that no protective effect was detectable at earlier time points is not surprising in view of the rapid decrease in tumour red cell flux and perfusion index induced by Y27632 alone. These vascular effects are most likely driven by the hypotensive effect of Y27632, resulting primarily from relaxation of vascular

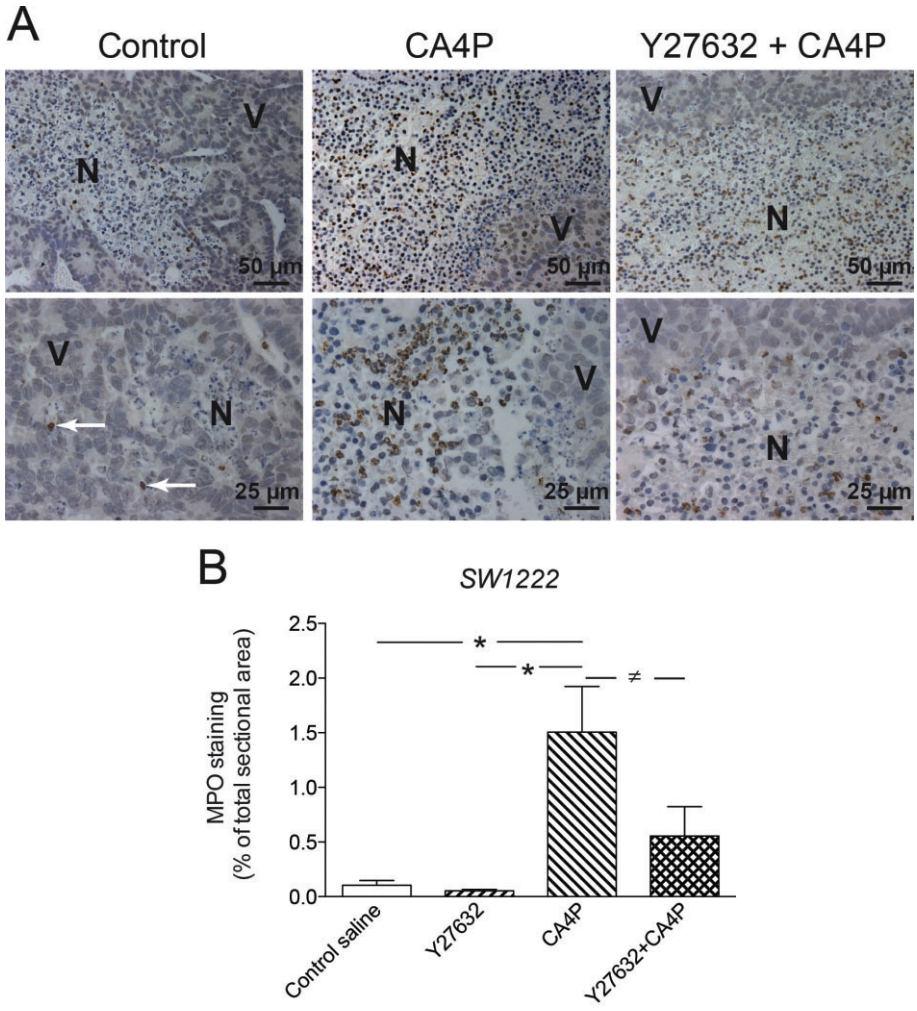

Figure 5

(A) Representative images of MPO immuno-staining (brown) in control untreated SW1222 tumours, 24 h after CA4P (100 mg kg^{-1}) alone and 24 h after the combination treatment with Y27632 (50 mg kg^{-1}) administered 5 min prior to CA4P. Staining in tumours exposed to Y27632 alone was very similar to that in controls (image not shown). White arrows indicate representative individual positively stained cells in a viable region of a control tumour. V represents viable and N represents necrotic tumour tissue. (B) Quantified data for all four groups. Columns represent means ± SEM for $n = 8$ per group. *$P < 0.05$ significant difference between groups; one-way ANOVA with Bonferroni post test. The difference between the CA4P group and the combination group was borderline significant (≠) depending on the *post hoc* test used (see main text for details).

smooth muscle cells in resistance arterioles of normal tissues (Ito *et al.*, 2003; Moosmang *et al.*, 2003), which follows the same time course as the tumour perfusion index, recovering to control levels between 3 and 5 h (comparing Figures 2A and 3B). There was also no additive effect of the early decreases in red cell flux or perfusion index observed for Y27632 and CA4P alone, when the two drugs were combined (Figure 2B and 3B), suggesting a protective interaction between the two drugs. In any case, once the hypotensive and blood flow modifying effects of Y27632 alone resolved, a protective effect of Y27632 against the vascular disrupting effects of CA4P was clearly apparent (6 and 24 h time points in Figure 3B), whereas no such effect was found for hydralazine, despite this drug having a similar hypotensive profile. The tumour vascular disrupting activity of CA4P is not only due to a vasoconstrictive effect on supplying arterioles (which also occurs in a range of normal tissues, accounting for the mild hypertensive effect of the drug) but also to direct damage to tumour endothelial cells (reviewed in Tozer *et al.*, 2008b). The fact that hydralazine did not protect against CA4P-induced tumour vascular disruption and necrosis strongly suggests that the protective effect of Y27632 is due to blocking of ROCK-mediated cytoskeletal damage to tumour endothelial cells. Staining for p-ERM showed a CA4P-induced expression in tumour cells, as well as in tumour vasculature, that was blocked by Y27632 treatment. However, by utilizing SW1222 tumour cells developed to be resistant to CA4P, we have previously shown that the anti-tumour activity of CA4P *in vivo* is mediated by its tumour vascular effects, rather than by direct toxicity towards the tumour cells themselves (Lunt *et al.*, 2011).

Although significant, the protective effects of Y27632 were only partial, suggesting that CA4P-induced tumour vascular disruption is not totally ROCK dependent. The fact that

the hypotensive effect of Y27632 had worn off after 3 to 5 h is consistent with a short plasma half-life for Y27632 in mice (van Beuge *et al.*, 2011). This suggests that, when given before CA4P, the drug interacts with CA4P-induced effects that occur within the first few hours following treatment, which results in partial protection from CA4P-induced tumour vascular damage that is manifested when the hypotensive effect of Y27632 has worn off. In order to check whether ROCK inhibition could protect against later effects, Y27632 was also administered 3 h after CA4P but, under these conditions, it had no significant vascular protective effect. This supports the notion that Y27632 is acting at an early stage in the vascular disruptive process and is consistent with the known activity of Y27632 in endothelial cells *in vitro*, where it prevents the CA4P-induced cytoskeletal remodelling, cell shape changes and increase in monolayer permeability to macromolecules that occur within 30 minutes of drug exposure (Kanthou and Tozer, 2002). However, we cannot exclude the possibility that drug access problems at 3 h after CA4P treatment could explain the lack of any significant effect when Y27632 was administered at this later time point.

I-R injury, as tumour blood vessels dilate following initial CA4P-induced collapse and blood flow struggles to re-establish, is likely to contribute to the outcome of VDA treatment. As noted above, ROCK is strongly activated during I-R in the heart and inhibition of ROCK can attenuate the consequent injury and inflammation (Bao *et al.*, 2004; Hamid *et al.*, 2007). Thus, the partial protective effect of Y27632 administration against CA4P, in our study, could involve protection against I-R injury. ROCK was found to cause injury by inactivating pro-survival signalling via PI3K/AKT and endothelial NOS (eNOS), thus limiting NO bioavailability (Rikitake *et al.*, 2005; Hamid *et al.*, 2007). This mechanism may apply to tumours, as NOS inhibition has been shown to exacerbate the vascular damaging effects of CA4P (Tozer *et al.*, 2009). The role of neutrophils in I-R injury is well established, with neutrophil-associated MPO contributing to production of damaging free radicals (Rodrigues and Granger, 2010). Here, we showed that ROCK inhibition was associated with a substantially decreased CA4P-induced MPO expression, which is consistent with the known role of ROCK activation in mediating neutrophil migration and endothelial adhesion (Alblas *et al.*, 2001; Saito *et al.*, 2002). However, such an association provides no information on cause and effect and since MPO is expressed in activated macrophages and other granulocyte lineage populations, as well as neutrophils (Tavora *et al.*, 2009), we cannot exclude the involvement of other cell types here. Recent evidence has shown that the net result of Tie2 + macrophage infiltration following CA4P treatment is to decrease the final elicited damage (Welford *et al.*, 2011). Similar experiments need to be carried out, ideally in immune-competent mice, to determine whether I/R injury associated with neutrophil infiltration acts to increase VDA-induced tumour vascular damage or whether the net effect is a more rapid recovery via a stimulation of angiogenesis.

In SW1222 tumours, the protective effect of Y27632 was translated into a protective effect on CA4P-induced necrosis. However, this was not the case for the LS174T tumour, in which Y27632 caused a similar protective effect against CA4P-induced vascular damage as it did in the SW1222 tumours but had no effect on necrosis induction. This is not surprising in view of the very high levels of necrosis already present in untreated LS174T tumours, which CA4P treatment did not affect. Untreated LS174T tumours are also very hypoxic (Professor R Barbara Pedley, University College London, pers. comm.) suggesting that CA4P may be ineffective against them, in terms of necrosis induction, because the tumour cells are adapted to survival under hypoxic conditions. A higher dose of CA4P than used here has previously been reported to increase necrosis in LS174T tumours but to a much lesser extent than in SW1222 tumours (Pedley *et al.*, 2002), which is consistent with our result.

We have found that activation of the Rho/ROCK signalling pathway plays an important role in the vascular disrupting action of CA4P *in vivo*, which translates into necrosis induction in CA4P-responsive tumours. It is likely that this is also the case for closely related drugs currently in clinical trial, such as Oxi4503 and ombrabulin. Since increased ROCK is known to exacerbate injury in other disease states via inactivation of pro-survival signalling via PI3K/AKT and eNOS, the current data provides a mechanistic explanation for the efficacy of combining NOS inhibition with CA4P. It also provides a rationale for investigating pharmacological intervention at other points in the pro-survival pathway for therapeutic benefit in combination with VDAs. The current results suggest that other classes of agents that activate Rho/ROCK signalling have potential as VDAs, such that this signalling pathway could form the basis of a useful drug screen.

Acknowledgements

We thank OxiGene Inc. for supply of CA4P and Professor R. B. Pedley for providing the SW1222 tumour cell line and for very useful discussion of the data. We thank Dr E. El-Emir and Professor Pedley for the protocol for use of tomato lectin and staff at the University of Sheffield for care of the animals. We thank Cancer Research UK (grant reference numbers C1276/A9993 and STU/C1276) and Yorkshire Cancer Research (grant reference number S307) for funding this research.

Author contributions

L. J. W. and D.M. contributed to experimental design, data collection, analysis and manuscript preparation; M. F. contributed to experimental design, data collection and analysis; C-C. Reyes-Aldasoro contributed to data analysis; S. Akerman contributed to data collection; C. K. and G. M. T. conceived and had overall responsibility for the project and contributed to experimental design, data analysis and manuscript preparation. G. M. T. was responsible for finalizing the manuscript.

Conflict of interest

The authors declare that there are no conflicts of interest associated with this manuscript.

References

Alblas J, Ulfman L, Hordijk P, Koenderman L (2001). Activation of RhoA and ROCK are essential for detachment of migrating leukocytes. Mol Biol Cell 12: 2137–2145.

Alexander SPH, Benson HE, Faccenda E, Pawson AJ, Sharman JL, Spedding M *et al.* (2013). The Concise Guide to PHARMACOLOGY 2013/14: Enzymes. British Journal of Pharmacology, 170: 1797–1867.

Bao W, Hu E, Tao L, Boyce R, Mirabile R, Thudium DT *et al.* (2004). Inhibition of Rho-kinase protects the heart against ischemia/reperfusion injury. Cardiovasc Res 61: 548–558.

van Beuge MM, Prakash J, Lacombe M, Post E, Reker-Smit C, Beljaars L *et al.* (2011). Increased liver uptake and reduced hepatic stellate cell activation with a cell-specific conjugate of the Rho-kinase inhibitor Y27632. Pharmaceut Res 28: 2045–2054.

Boehle AS, Sipos B, Kliche U, Kalthoff H, Dohrmann P (2001). Combretastatin A-4 prodrug inhibits growth of human non-small cell lung cancer in a murine xenotransplant model. Ann Thorac Surg 71: 1657–1665.

Dark GD, Hill SA, Prise VE, Tozer GM, Pettit GR, Chaplin DJ (1997). Combretastatin A-4, an agent that displays potent and selective toxicity toward tumor vasculature. Cancer Res 57: 1829–1834.

Dowlati A, Robertson K, Cooney M, Petros WP, Stratford M, Jesberger J *et al.* (2002). A phase I pharmacokinetic and translational study of the novel vascular targeting agent combretastatin a-4 phosphate on a single-dose intravenous schedule in patients with advanced cancer. Cancer Res 62: 3408–3416.

Fehon RG, McClatchey AI, Bretscher A (2010). Organizing the cell cortex: the role of ERM proteins. Nat Rev Mol Cell Biol 11: 276–287.

Galbraith SM, Maxwell RJ, Lodge MA, Tozer GM, Wilson J, Taylor NJ *et al.* (2003). Combretastatin A4 phosphate has tumor antivascular activity in rat and man as demonstrated by dynamic magnetic resonance imaging. J Clin Oncol 21: 2831–2842.

Hamid SA, Bower HS, Baxter GF (2007). Rho kinase activation plays a major role as a mediator of irreversible injury in reperfused myocardium. Am J Physiol Heart Circ Physiol 292: H2598–H2606.

Hill SA, Chaplin DJ, Lewis G, Tozer GM (2002). Schedule dependence of combretastatin A4 phosphate in transplanted and spontaneous tumour models. Int J Cancer 102: 70–74.

Ito K, Hirooka Y, Sakai K, Kishi T, Kaibuchi K, Shimokawa H *et al.* (2003). Rho/Rho-kinase pathway in brain stem contributes to blood pressure regulation via sympathetic nervous system: possible involvement in neural mechanisms of hypertension. Circ Res 92: 1337–1343.

Kanthou C, Tozer GM (2002). The tumor vascular targeting agent combretastatin A-4-phosphate induces reorganization of the actin cytoskeleton and early membrane blebbing in human endothelial cells. Blood 99: 2060–2069.

Kanthou C, Tozer GM (2007). Tumour targeting by microtubule-depolymerizing vascular disrupting agents. Exp Opin Ther Targets 11: 1443–1457.

Ke Q, Bodyak N, Rigor DL, Hurst NW, Chaplin DJ, Kang PM (2009). Pharmacological inhibition of the hypertensive response to combretastatin A-4 phosphate in rats. Vasc Pharmacol 51: 337–343.

Kilkenny C, Browne W, Cuthill IC, Emerson M, Altman DG (2010). Animal research: reporting in vivo experiments: the ARRIVE guidelines. Br J Pharmacol 160: 1577–1579.

Lunt SJ, Akerman S, Hill SA, Fisher M, Wright VJ, Reyes-Aldasoro CC *et al.* (2011). Vascular effects dominate solid tumor response to treatment with combretastatin A-4-phosphate. Int J Cancer 129: 1979–1989.

Matsui T, Maeda M, Doi Y, Yonemura S, Amano M, Kaibuchi K *et al.* (1998). Rho-kinase phosphorylates COOH-terminal threonines of ezrin/radixin/moesin (ERM) proteins and regulates their head-to-tail association. J Cell Biol 140: 647–657.

Mavria G, Vercoulen Y, Yeo M, Paterson H, Karasarides M, Marais R *et al.* (2006). ERK-MAPK signaling opposes Rho-kinase to promote endothelial cell survival and sprouting during angiogenesis. Cancer Cell 9: 33–44.

McGown AT, Fox BW (1989). Structural and biochemical comparison of the anti-mitotic agents colchicine, combretastatin A4 and amphethinile. Anticancer Drug Des 3: 249–254.

McGrath J, Drummond G, McLachlan E, Kilkenny C, Wainwright C (2010). Guidelines for reporting experiments involving animals: the ARRIVE guidelines. Br J Pharmacol 160: 1573–1576.

van der Meel R, Symons MH, Kudernatsch R, Kok RJ, Schiffelers RM, Storm G *et al.* (2011). The VEGF/Rho GTPase signalling pathway: a promising target for anti-angiogenic/anti-invasion therapy. Drug Discov Today 16: 219–228.

Moosmang S, Schulla V, Welling A, Feil R, Feil S, Wegener JW *et al.* (2003). Dominant role of smooth muscle L-type calcium channel Cav1.2 for blood pressure regulation. EMBO J 22: 6027–6034.

Murata R, Overgaard J, Horsman MR (2001a). Comparative effects of combretastatin A-4 disodium phosphate and 5,6-dimethylxanthenone-4-acetic acid on blood perfusion in a murine tumour and normal tissues. Int J Radiat Biol 77: 195–204.

Murata R, Siemann DW, Overgaard J, Horsman HR (2001b). Interaction between combretastatin A-4 disodium phosphate and radiation in murine tumors. Radiother Oncol 60: 155–161.

Nathan P, Zweifel M, Padhani AR, Koh DM, Ng M, Collins DJ *et al.* (2012). Phase I trial of combretastatin A4 phosphate (CA4P) in combination with bevacizumab in patients with advanced cancer. Clin Cancer Res 18: 3428–3439.

Orian-Rousseau V, Ponta H (2008). Adhesion proteins meet receptors: a common theme? Adv Cancer Res 101: 63–92.

Parkins CS, Holder AJ, Hill SA, Chaplin DJ, Tozer GM (2000). Determinants of anti-vascular action by combretastatin A-4 phosphate: role of nitric oxide. Br J Cancer 83: 811–816.

Pawson AJ, Sharman JL, Benson HE, Faccenda E, Alexander SP, Buneman OP, Davenport AP, McGrath JC, Peters JA, Southan C, Spedding M, Yu W, Harmar AJ; NC-IUPHAR. (2014). The IUPHAR/BPS Guide to PHARMACOLOGY: an expert-driven knowledge base of drug targets and their ligands. Nucl. Acids Res 42 (Database Issue): D1098–1106.

Pedley RB, El-Emir E, Flynn AA, Boxer GM, Dearling J, Raleigh JA *et al.* (2002). Synergy between vascular targeting agents and antibody-directed therapy. Int J Radiat Oncol Biol Phys 54: 1524–1531.

Pettit GR, Singh SB, Hamel E, Lin CM, Alberts DS, Garia-Kendall D (1989). Isolation and structure of the strong cell growth and tubulin inhibitor combretastatin A4. Experientia 45: 205–211.

Pettit GR, Temple C, Narayanan VL, Varma R, Simpson MJ, Boyd MR *et al.* (1995). Antineoplastic agents 322. Synthesis of combretastatin A-4 prodrugs. Anticancer Drug Des 10: 299–309.

Prise VE, Honess DJ, Stratford MRL, Wilson J, Tozer GM (2002). The vascular response of tumor and normal tissues in the rat to the

vascular targeting agent, combretastatin A-4-phosphate, at clinically relevant doses. Int J Oncol 21: 717–726.

Reyes-Aldasoro CC, Wilson I, Prise VE, Barber PR, Ameer-Beg SM, Vojnovic B *et al*. (2008). Estimation of apparent tumor vascular permeability from multiphoton fluorescence microscopic images of P22 rat sarcomas in vivo. Microcirculation 15: 65–79.

Richman PI, Bodmer WF (1988). Control of differentiation in human colorectal carcinoma cell lines: epithelial-mesenchymal interactions. J Pathol 156: 197–211.

Rikitake Y, Kim HH, Huang Z, Seto M, Yano K, Asano T *et al*. (2005). Inhibition of Rho kinase (ROCK) leads to increased cerebral blood flow and stroke protection. Stroke 36: 2251–2257.

Rodrigues SF, Granger DN (2010). Role of blood cells in ischaemia-reperfusion induced endothelial barrier failure. Cardiovasc Res 87: 291–299.

Rustin GJ, Galbraith SM, Anderson H, Stratford M, Folkes LK, Sena L *et al*. (2003). Phase I clinical trial of weekly combretastatin A4 phosphate: clinical and pharmacokinetic results. J Clin Oncol 21: 2815–2822.

Saito H, Minamiya Y, Saito S, Ogawa J (2002). Endothelial Rho and Rho kinase regulate neutrophil migration via endothelial myosin light chain phosphorylation. J Leukoc Biol 72: 829–836.

Sawada N, Itoh H, Ueyama K, Yamashita J, Doi K, Chun TH *et al*. (2000). Inhibition of rho-associated kinase results in suppression of neointimal formation of balloon-injured arteries. Circulation 101: 2030–2033.

Shaked Y, Ciarrocchi A, Franco M, Lee CR, Man S, Cheung AM *et al*. (2006). Therapy-induced acute recruitment of circulating endothelial progenitor cells to tumors. Science 313: 1785–1787.

Shaked Y, Tang T, Woloszynek J, Daenen LG, Man S, Xu P *et al*. (2009). Contribution of granulocyte colony-stimulating factor to the acute mobilization of endothelial precursor cells by vascular disrupting agents. Cancer Res 69: 7524–7528.

Sheng Y, Hua J, Pinney KG, Garner CM, Kane RR, Prezioso JA *et al*. (2004). Combretastatin family member OXI4503 induces tumor vascular collapse through the induction of endothelial apoptosis. Int J Cancer 111: 604–610.

Siemann DW (2011). The unique characteristics of tumor vasculature and preclinical evidence for its selective disruption by tumor-vascular disrupting agents. Cancer Treat Rev 37: 63–74.

Siemann DW, Shi W (2008). Dual targeting of tumor vasculature: combining Avastin and vascular disrupting agents (CA4P or OXi4503). Anticancer Res 28 (4B): 2027–2031.

Siemann DW, Mercer E, Lepler S, Rojiani AM (2002). Vascular targeting agents enhance chemotherapeutic agent activities in solid tumor therapy. Int J Cancer 99: 1–6.

Stratford MR, Dennis MF (1999). Determination of combretastatin A-4 and its phosphate ester pro-drug in plasma by high-performance liquid chromatography. J Chromat B, Biomed Sci App 721: 77–85.

Tavora FR, Ripple M, Li L, Burke AP (2009). Monocytes and neutrophils expressing myeloperoxidase occur in fibrous caps and thrombi in unstable coronary plaques. BMC Cardiovasc Dis 9: 27.

Tozer GM, Prise VE, Wilson J, Locke RJ, Vojnovic B, Stratford MRL *et al*. (1999). Combretastatin A-4 phosphate as a tumor vascular-targeting agent: early effects in tumors and normal tissues. Cancer Res 59: 1626–1634.

Tozer GM, Kanthou C, Baguley BC (2005). Disrupting tumour blood vessels. Nat Rev Cancer 5: 423–435.

Tozer GM, Akerman S, Cross NA, Barber PR, Bjorndahl MA, Greco O *et al*. (2008a). Blood vessel maturation and response to vascular-disrupting therapy in single vascular endothelial growth factor-A isoform-producing tumors. Cancer Res 68: 2301–2311.

Tozer GM, Kanthou C, Lewis G, Prise VE, Vojnovic B, Hill SA (2008b). Tumour vascular disrupting agents: combating treatment resistance. Br J Radiol 81 (Spec1): S12–S20.

Tozer GM, Prise VE, Lewis G, Xie S, Wilson I, Hill SA (2009). Nitric oxide synthase inhibition enhances the tumor vascular-damaging effects of combretastatin a-4 3-O-phosphate at clinically relevant doses. Clin Cancer Res 15: 3781–3790.

Uehata M, Ishizaki T, Satoh H, Ono T, Kawahara T, Morishita T *et al*. (1997). Calcium sensitization of smooth muscle mediated by a Rho-associated protein kinase in hypertension. Nature (London) 389: 990–994.

Vincent L, Kermani P, Young LM, Cheng J, Zhang F, Shido K *et al*. (2005). Combretastatin A4 phosphate induces rapid regression of tumor neovessels and growth through interference with vascular endothelial-cadherin signaling. J Clin Invest 115: 2992–3006.

Wang L, Ellis MJ, Fields TA, Howell DN, Spurney RF (2008). Beneficial effects of the Rho kinase inhibitor Y27632 in murine puromycin aminonucleoside nephrosis. Kidney Blood Pressure Res 31: 111–121.

Welford AF, Biziato D, Coffelt SB, Nucera S, Fisher M, Pucci F *et al*. (2011). TIE2-expressing macrophages limit the therapeutic efficacy of the vascular-disrupting agent combretastatin A4 phosphate in mice. J Clin Invest 121: 1969–1973.

Workman P, Aboagye EO, Balkwill F, Balmain A, Bruder G, Chaplin DJ *et al*. (2010). Guidelines for the welfare and use of animals in cancer research. Br J Cancer 102: 1555–1577.

Supporting information

Additional Supporting Information may be found in the online version of this article at the publisher's web-site:

http://dx.doi.org/10.1111/bph.12817

Figure S1 Perfusion index calculated as the number of pixels stained + ve for FITC-lectin as a % of the number of pixels stained + ve for CD31 at 6 and 24 h after CA4P for CA4P alone group and for Y27632 administered 3 h after CA4P ($n > 8$ for all groups). Points represent means ± 1 SEM. There was no significant difference between CA4P alone and CA4P + Y27632 at either time point (two-way ANOVA with Bonferroni post test).

Appendix S1 Supplementary methods.